

GuiDINO: Rethinking Vision Foundation Model in Medical Image Segmentation

Zhuonan Liang¹, Wei Guo¹, Jie Gan¹, Yaxuan Song¹, Runnan Chen¹, Hang Chang^{2,3}, and Weidong Cai¹

¹ The University of Sydney, Sydney. NSW 2006, Australia

² Biological System & Engineering Division, Lawrence Berkeley National Laboratory, Berkeley. CA 94720, USA

³ Berkeley Biomedical Data Science Center, Lawrence Berkeley National Laboratory, Berkeley. CA 94720, USA
tom.cai@sydney.edu.au

Abstract. Foundation vision models are increasingly adopted in medical image analysis. Due to domain shift, these pretrained models misalign with medical image segmentation needs without being fully fine-tuned or lightly adapted. We introduce GuiDINO, a framework that repositions native foundation model to acting as a visual guidance generator for downstream segmentation. GuiDINO extracts visual feature representation from DINOv3 and converts them into a spatial guide mask via a lightweight TokenBook mechanism, which aggregates token-prototype similarities. This guide mask gates feature activations in multiple segmentation backbones, thereby injecting foundation-model priors while preserving the inductive biases and efficiency of medical dedicated architectures. Training relies on a guide supervision objective loss that aligns the guide mask to ground-truth regions, optionally augmented by a boundary-focused hinge loss to sharpen fine structures. GuiDINO also supports parameter-efficient adaptation through LoRA on the DINOv3 guide backbone. Across diverse medical datasets and nnUNet-style inference, GuiDINO consistently improves segmentation quality and boundary robustness, suggesting a practical alternative to fine-tuning and offering a new perspective on how foundation models can best serve medical vision. Code is available at <https://github.com/Hi-FishU/GuiDINO>.

Keywords: Medical Image Analysis · Foundation Models · Segmentation · DINO · TokenBook.

1 Introduction

Vision foundation models (VFMs) have revolutionized computer vision by learning rich, generalizable representations from large-scale data [21, 18, 10, 15]. Token-based VFMs, such as DINOv3, have shown remarkable capabilities in learning dense representations that capture both global and local image features, which can potentially boost the generalizabilities of dedicated medical image segmentation networks [18, 21, 26, 28]. However, the semantic features of tokens are not

directly aligned with medical tasks [25, 26, 15]. To mitigate the scenarios shift, the straightforward solution is fine-tuning VFMs. However, it may also require extensive computational resources and large annotated datasets compared with traditional medical imaging models, which are scarce in the medical domain [17]. From the other perspective, the dedicated designs of medical image segmentation architectures have been shown to be effective in capturing the specific features of medical images, including convolution-based and transformer-based variants [12, 19, 30, 8, 27].

Therefore, this raises the question of how the vision foundation model benefits medical image segmentation on the well-developed designs? Despite semantic gap exists, these tokens still can potentially provide valuable visual guidance for segmentation tasks without the need for full fine-tuning. The concept of using guidance for segmentation has been explored in various contexts, such as interactive segmentation and weakly supervised segmentation [23, 22, 29, 20]. However, the idea of using native foundation models as guidance generators for medical image segmentation is relatively unexplored. By leveraging the rich token representations from foundation models, we can efficiently guide the segmentation process while preserving the inductive biases of medical image segmentation architectures. The insights of this approach are twofold: (1) Foundation models can serve as powerful extractors that only provide spatial guidance on visual features rather than suffering from semantic discrepancy; (2) The dedicated medical network can focus on learning the semantic features relevant to medical images without being burdened by the need to adapt to the general representations.

That raises a question: how to effectively utilize the token features from foundation models to guide medical image segmentation? To address this, we propose Guided-by-DINO (GuiDINO), a novel framework leverages the generalizabilities of VFMs on visual representation to spatially guide the dedicate medical network training. GuiDINO extracts visual features representation by natively pretrained DINOv3 and then converts them into a spatial guide mask via a lightweight TokenBook mechanism, which aggregates token-prototype similarities. This guide mask gates feature activations in multiple segmentation backbones, thereby injecting foundation-model priors while preserving the semantic biases and efficiency of medical image segmentation architectures. Training combines standard segmentation losses with a guide supervision objective that aligns the guide mask to ground-truth regions, optionally augmented by a boundary-focused hinge loss to sharpen fine structures. GuiDINO also supports parameter-efficient adaptation through LoRA on the DINOv3 guide backbone. Overall, our contributions are as follows:

1. We provide a novel insightful perspective on the role of foundation models in medical image segmentation, advocating for their use as spatial guidance generators as enhancing spatial recognizabilities.
2. We propose the GuiDINO framework with TokenBook mechanism, which effectively leverages token features from DINOv3 to create spatial masks that guide segmentation while maintaining the efficiency and inductive biases of medical image segmentation architectures.

3. We demonstrate the effectiveness of GuiDINO across diverse medical datasets, showing consistent improvements in segmentation performance and boundary delineation compared to traditional backbone fine-tuning approaches.

2 Related Works

Recent advances in medical image segmentation have increasingly explored the use of vision foundation models such as self-supervised DINO variants [26, 14] and the Segment Anything family [23, 16, 22, 1], leveraging the rich semantic representations learned from large, diverse natural image corpora. In medical image analysis, these models hold promise for improving segmentation tasks, which are critical for diagnosis and treatment planning [26, 22, 16, 7]. However, the common practice of introducing foundation models as backbones for segmentation often overlooks the unique challenges of medical imaging, such as the need for precise boundary delineation, and significant modality shifts [17, 3]. This can lead to suboptimal performance and inefficient training. Numerous works have evaluated the transferability and zero-shot capabilities of these foundation models in medical domains, highlighting both potential and challenges: foundation models demonstrate significant generalization across modalities in zero-shot scenarios but often underperform without adaptation due to domain gap and structural differences between natural and clinical images [17, 11, 13, 7]. Early adaptation strategies focused on fine-tuning VFMs or designing hybrid architectures that combine foundation backbones with task-specific decoders, showing improved performance at the cost of heavy supervision or prompt engineering [1, 23, 22]. Parallel efforts on DINO-based adaptation have led to methods like MedDINOv3 and SegDINO, which explore multi-scale token aggregation and lightweight decoders together with frozen DINO backbones to balance efficiency and accuracy in segmentation tasks [26, 25]. Other research has examined the applicability of frozen foundation features for related dense prediction tasks and found that fixed representations can support training-free or test-time optimization strategies [24]. Despite these advances, most approaches still involve optimization of task-specific parameters, adapters, or extensive data requirements, leaving a gap for lightweight integration of pretrained tokens without any backbone fine-tuning. Our work aims to address this gap by designing a segmentation head that directly exploits frozen token semantics from foundation models, preserving pretrained generalization while minimizing training complexity and avoiding adaptation of backbone weights.

3 Methods

In this section, we describe the proposed GuiDINO framework in detail. We first provide an overview of the architecture and then delve into the specific components, including the TokenBook mechanism for generating guide masks and the training objectives used to optimize the model. The GuiDINO pipeline consists of three main components: (1) a natural pretrained guide generator that

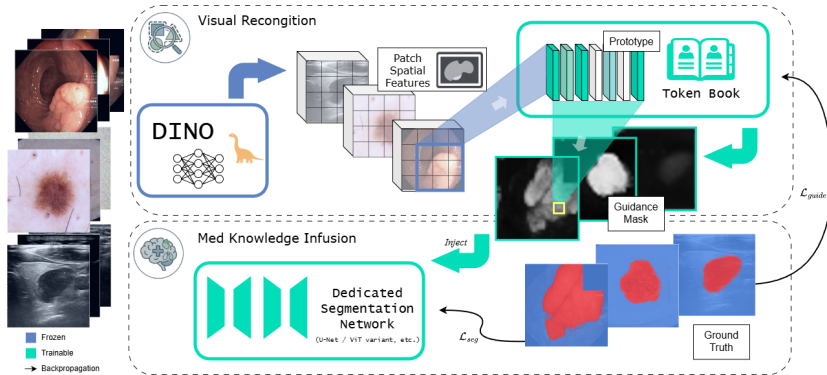


Fig. 1. Overview of the proposed GuiDINO framework. The frozen DINOv3 backbone serves as a guide generator, extracting dense token features that are converted into spatial guide masks via the TokenBook mechanism. These guide masks are then used to gate feature activations in the segmentation backbone, which produces the final segmentation output.

extracts dense token features and converts them into spatial guide masks, (2) a complete segmentation backbone that takes the original image and the guide mask as input to produce the final segmentation output, and (3) a training framework that combines standard segmentation losses with guide supervision objectives to optimize both the guide generator and the segmentation backbone. We take DINOv3 as the default guide generator, but our framework is flexible to accommodate other token-based visual foundation models as well. Overview of the architecture is shown in Figure 1.

3.1 TokenBook for Guide Mask Generation

The frozen backbone encoder is pretrained on the natural image datasets, which is not directly aligned with the medical image segmentation task. To bridge this gap, we introduce a lightweight TokenBook mechanism that converts prior token features into spatial guide masks. The TokenBook aggregates token-prototype similarities to create a spatial map that highlights regions of interest for segmentation:

$$G(x) = \sum_{i=1}^N \alpha_i \cdot \text{sim}(T_i, P), \quad (1)$$

where $G(x)$ is the guide mask for the input image x , T_i represents the token features extracted from the backbone, P denotes a set of learned prototypes that capture relevant visual patterns, and α_i are learnable weights that determine the contribution of each token to the guide mask. The similarity function $\text{sim}(\cdot)$ can be implemented as a dot product or cosine similarity, depending on the specific design choice. By learning the prototypes and weights, the TokenBook can effectively translate the general token features into a spatial guide that is

more aligned with the medical image segmentation task. The resulting guide mask is then used to gate feature activations in the segmentation backbone, allowing the model to focus on relevant regions while preserving the inductive biases of the medical image segmentation architecture.

3.2 Learning Objectives

To integrate semantic token priors from the DINO backbone with dense prediction supervision, we adopt a composite training objective that couples a segmentation loss with a guide-alignment regularization term. This design enforces consistency between the segmentation decoder and the auxiliary guide branch.

The overall loss function can be expressed as:

$$\mathcal{L} = \mathcal{L}_{\text{seg}} + \lambda \mathcal{L}_{\text{guide}}, \quad (2)$$

where \mathcal{L}_{seg} is the standard segmentation loss (e.g., Dice loss or cross-entropy loss) that measures the discrepancy between the predicted segmentation mask and the ground-truth. The term $\mathcal{L}_{\text{guide}}$ is a guide supervision objective that encourages the generated guide mask to align with the ground-truth segmentation regions. This can be implemented as a binary cross-entropy loss between the guide mask and the ground-truth mask:

$$\mathcal{L}_{\text{guide}} = -\frac{1}{N} \sum_{i=1}^N [y_i \log(g_i) + (1 - y_i) \log(1 - g_i)], \quad (3)$$

where y_i is the ground truth label for pixel i , and g_i is the corresponding value in the guide mask. The hyperparameter λ controls the relative importance of the guide supervision term. By optimizing this composite loss, we can ensure that the guide mask effectively captures relevant features that contribute to improved segmentation performance. Additionally, to further enhance boundary delineation, we can optionally include a boundary-focused hinge loss that penalizes discrepancies between the predicted segmentation boundaries and the ground truth, encouraging sharper and more accurate segmentation results.

4 Experiments and Results

4.1 Datasets and Evaluation Metrics

The experiments are conducted on several publicly available medical imaging datasets, including Kvasir [9], ISIC [4], and TK3N [5]. **Kvasir-SEG** consists of 1,000 colonoscopy images with corresponding pixel-level binary masks for polyp segmentation. Image resolutions vary across samples. **ISIC 2017** contains 2,750 dermoscopic images with expert-annotated lesion masks. **TN3K** includes 3,493 thyroid ultrasound images from 2,421 patients with pixel-level nodule annotations. These datasets cover a range of medical imaging modalities and segmentation tasks, providing a comprehensive evaluation of the proposed GuiDINO

Table 1. Baseline results on Kvasir-SEG, ISIC2017, and TN3K datasets.

Method	Kvasir-SEG			ISIC 2017			TN3K		
	IoU \uparrow	DSC \uparrow	HD95 \downarrow	IoU \uparrow	DSC \uparrow	HD95 \downarrow	IoU \uparrow	DSC \uparrow	HD95 \downarrow
nnUNet [8]	83.92	89.71	20.85	82.30	89.18	13.38	72.81	82.38	33.47
SwinUNet [2]	–	–	–	81.24	88.38	14.17	–	–	–
H2Former [6]	83.87	89.50	19.81	82.56	89.36	13.04	–	–	–
U-KAN [12]	63.81	72.17	36.92	74.62	83.41	23.57	69.60	78.66	24.49
nnWNet [30]	84.58	89.98	18.17	82.62	89.44	12.73	66.46	76.02	38.61
SegDINO [26]	80.64	87.65	18.62	77.60	85.76	20.80	74.43	83.18	18.62
GuiDINO-W	84.82	90.86	17.50	82.32	89.81	13.14	74.48	83.40	24.80

framework. We use standard evaluation metrics for medical image segmentation, including Dice coefficient, Intersection over Union (IoU), and HD95 Score, to assess the performance of our model.

4.2 Implementation Details

We implement the GuiDINO framework using PyTorch. The DINOv3 backbone is initialized with pretrained weights from official repo⁴. The DINOv3 is kept frozen during training, while the TokenBook and segmentation backbone are trained from scratch. The input images are resized to a fixed resolution of 256x256 for training. We use the initial learning rate of 1e-4 and a batch size of 4. AdamW optimizer is applied in LoRA DINO optimization with 5e-4 learning rate. The model is trained for 400 epochs, and the best model is selected based on validation performance. Augmentation and inferences follow nnUNet [8] implementation. More details can be found in our project page⁵. The experiments are conducted on a single NVIDIA R6000 Ada GPU with 40GB of memory. All results are averaged over three runs with different random seeds to ensure robustness and reproducibility.

4.3 Experimental Results

To compare the performance of our proposed GuiDINO framework with existing methods, we evaluate several baseline models, including nnUNet [8], SwinUNet [2], H2Former [6], U-KAN [12], nnWNet [30], and SegDINO [26]. The results are summarized in Table 1. Our proposed GuiDINO framework applied on nnWNet (GuiDINO-W) outperforms the baseline models across all three datasets in terms of metrics. Notably, GuiDINO achieves the highest IoU and Dice scores on the Kvasir and ISIC datasets, demonstrating its effectiveness in improving segmentation performance. Additionally, GuiDINO shows competitive performance on the TN3K dataset, particularly in terms of HD95 Score, which indicates improved boundary delineation compared to other methods. These results highlight the potential of using foundation models as guidance generators for medical image segmentation tasks, offering a practical alternative to traditional backbone fine-tuning approaches.

⁴ <https://huggingface.co/facebook/dinov3-vits16-pretrain-lvd1689m>

⁵ <https://github.com/Hi-FishU/GuiDINO>

Table 2. Ablation of GuiDINO on different backbones across three datasets. Deltas in parentheses are relative to the corresponding backbone.

Method	Kvasir-SEG			ISIC 2017			TN3K		
	IoU \uparrow	DSC \uparrow	HD95 \downarrow	IoU \uparrow	DSC \uparrow	HD95 \downarrow	IoU \uparrow	DSC \uparrow	HD95 \downarrow
UNet backbone									
UNet [19]	70.29	79.16	41.58	72.95	81.87	41.58	70.65	79.45	24.59
GuiDINO-U	83.18 (+12.89)	89.51 (+10.35)	17.78 (-23.80)	81.24 (+8.29)	88.78 (+6.91)	17.86 (-23.72)	72.09 (+1.44)	81.41 (+1.96)	24.97 (+0.38)
nnWNet backbone									
nnWNet [30]	84.58	89.98	18.17	82.62	89.44	12.73	66.46	76.02	38.61
GuiDINO-W	84.82 (+0.24)	90.86 (+0.88)	17.50 (-0.67)	82.32 (-0.30)	89.81 (+0.37)	13.14 (+0.41)	74.48 (+8.02)	83.40 (+7.38)	24.80 (-13.81)

4.4 Ablation Study

We conduct an ablation study to evaluate the impact of the GuiDINO framework on different backbones across the three datasets. We compare the performance of the UNet and nnWNet backbones with and without the integration of GuiDINO. The results are presented in Table 2. The deltas in parentheses indicate the relative improvement compared to the corresponding backbone without GuiDINO. The results show that integrating GuiDINO consistently improves segmentation performance across both backbones and all datasets, with notable gains in IoU and Dice scores, as well as reductions in HD95 Score, indicating enhanced boundary accuracy. Notably, GuiDINO provides significant improvements when the backbone is burdened to suboptimal performance, such as in the case of nnWNet on TN3K and the UNet on ISIC 2017. This ablation study confirms the effectiveness of the GuiDINO framework in enhancing medical image segmentation by leveraging foundation model guidance while preserving the strengths of traditional segmentation architectures.

4.5 Discussion

We further compare the performance of Seg-DINO and Seg-GuiDINO variants with and without LoRA adaptation. The results are summarized in Table 3. The Seg-GuiDINO variant without LoRA shows a decrease in performance compared to Seg-DINO, which suggests that the guidance from DINO can be further refined by the LoRA adaptation. However, the promotion is not consistent across all datasets, indicating that the effectiveness of LoRA adaptation may depend on the specific characteristics of the dataset and the segmentation task. These results highlight the importance of both the guidance from DINO and the adaptation through LoRA in enhancing segmentation performance, while also suggesting that further research is needed to understand the conditions under which these components are most effective.

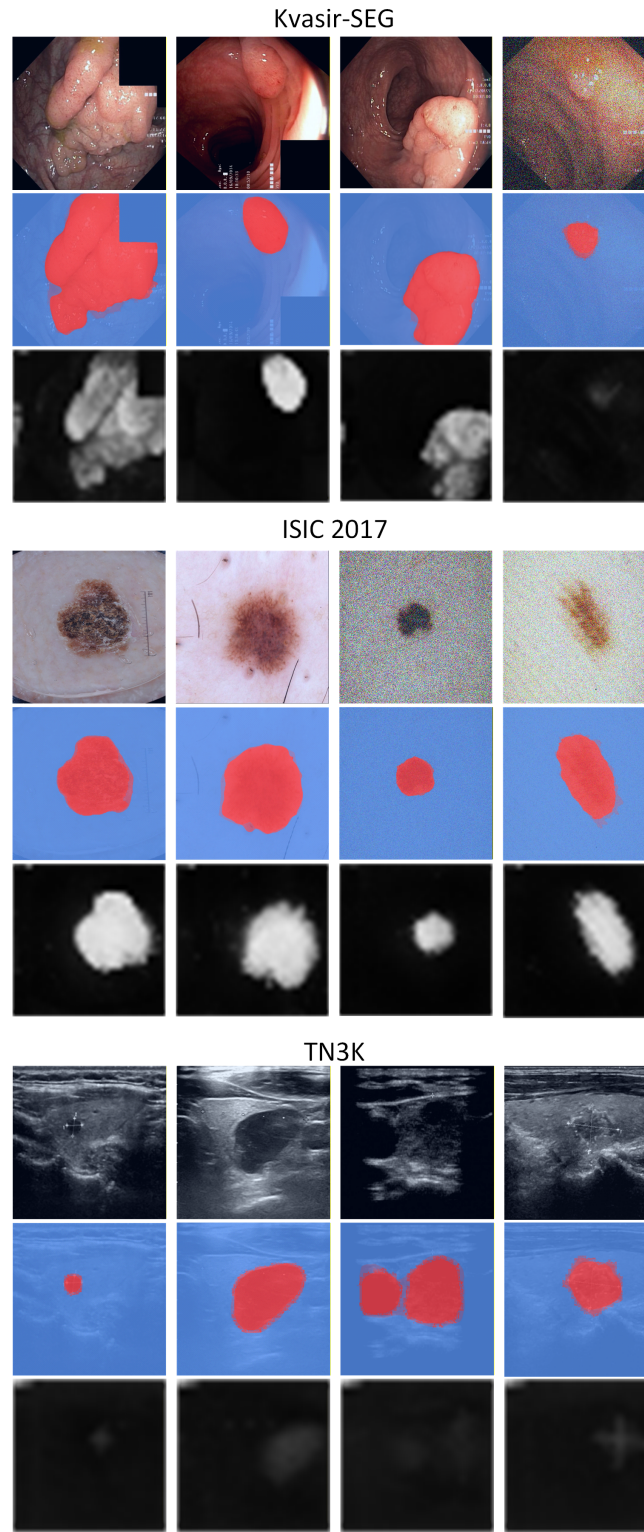


Fig. 2. Qualitative results for segmentation. **First row:** original input image. **Second row:** actual segmentation masks. **Third row:** guidance mask from GuiDINO. The guidance mask highlights the rough location of the target, which can assist the segmentation backbone in focusing on relevant regions.

Table 3. Comparison of Seg-DINO and GuiDINO-W variants (with/without LoRA).

Method	Kvasir			ISIC			TN3K		
	IoU \uparrow	DSC \uparrow	HD95 \downarrow	IoU \uparrow	DSC \uparrow	HD95 \downarrow	IoU \uparrow	DSC \uparrow	HD95 \downarrow
Seg-DINO [26]	80.64	89.65	18.62	77.60	85.76	20.80	74.43	83.18	18.62
Seg-GuiDINO	79.10	87.23	18.64	81.08	89.23	16.42	61.67	73.08	16.13
	(-1.54)	(-2.42)	(+0.02)	(+3.48)	(+3.47)	(-4.38)	(-12.76)	(-10.10)	(-2.51)
Seg-GuiDINO-LoRA	87.37	92.72	12.16	79.54	88.11	16.56	74.58	83.56	21.41
	(+6.73)	(+3.07)	(-6.46)	(+1.94)	(+2.35)	(-4.24)	(+0.15)	(+0.38)	(+2.79)
nnWNet [30]	84.58	89.98	18.17	82.62	89.44	12.73	66.46	76.02	38.61
GuiDINO-W	84.82	90.86	17.50	82.32	89.81	13.14	74.48	83.40	24.80
	(+0.24)	(+0.88)	(-0.67)	(-0.30)	(+0.37)	(+0.41)	(+8.03)	(+7.38)	(-13.81)
GuiDINO-W-LoRA	86.49	92.09	12.40	82.65	89.83	13.42	73.04	82.53	31.20
	(+1.91)	(+2.11)	(-5.77)	(+0.03)	(+0.40)	(+0.28)	(+6.58)	(+6.51)	(-7.41)

We visualize the guidance generated from DINO and compare with the actual mask of scope (as shown in Figure 2). It can be observed that the guidance from DINO can capture the rough location of the target, which can potentially help the segmentation backbone to focus on relevant regions, especially in challenging cases with low contrast or complex structures.

5 Conclusion

In this paper, we proposed GuiDINO, a novel framework that repositions vision foundation models as guidance generators for medical image segmentation tasks. GuiDINO effectively injects foundation-model priors into segmentation backbones while preserving their inductive biases. Our experiments on multiple datasets demonstrate that GuiDINO improves segmentation performance and boundary delineation compared to traditional backbone fine-tuning approaches. This work offers a new perspective on how foundation models can serve medical vision tasks as providing valuable guidance without the need for direct fine-tuning as backbones. Overall, GuiDINO represents a promising direction for leveraging foundation models in medical image analysis while maintaining efficiency and performance.

References

1. Archit, A., Freckmann, L., Pape, C.: Medicosam: Robust improvement of sam for medical imaging. *IEEE Transactions on Medical Imaging* **PP** (2025). <https://doi.org/10.1109/TMI.2025.3644811>, <https://www.ncbi.nlm.nih.gov/pubmed/41406266>
2. Cao, H., Wang, Y., Chen, J., Jiang, D., Zhang, X., Tian, Q., Wang, M.: Swin-unet: Unet-like pure transformer for medical image segmentation. In: *European conference on computer vision 2022*. pp. 205–218. *Computer Vision – ECCV 2022 Workshops*, Springer Nature Switzerland (2023). https://doi.org/10.1007/978-3-031-25066-8_9
3. Chen, Q., Liu, A., Zhang, J., Yang, C., Zhang, Y.: Foundation models in medical imaging: A review. *EngMedicine* **3**(2) (2026). <https://doi.org/10.1016/j.engmed.2026.100123>

4. Codella, N.C.F., Gutman, D., Celebi, M.E., Helba, B., Marchetti, M.A., Dusza, S.W., Kalloo, A., Liopyris, K., Mishra, N., Kittler, H., Halpern, A.: Skin lesion analysis toward melanoma detection: A challenge at the 2017 international symposium on biomedical imaging (isbi), hosted by the international skin imaging collaboration (isic). In: 2018 IEEE 15th International Symposium on Biomedical Imaging (ISBI 2018). pp. 168–172 (2018). <https://doi.org/10.1109/isbi.2018.8363547>
5. Gong, H., Chen, G., Wang, R., Xie, X., Mao, M., Yu, Y., Chen, F., Li, G.: Multi-task learning for thyroid nodule segmentation with thyroid region prior. In: 2021 IEEE 18th International Symposium on Biomedical Imaging (ISBI). pp. 257–261 (2021). <https://doi.org/10.1109/isbi48211.2021.9434087>
6. He, A., Wang, K., Li, T., Du, C., Xia, S., Fu, H.: H2former: An efficient hierarchical hybrid transformer for medical image segmentation. *IEEE Transactions on Medical Imaging* **42**(9), 2763–2775 (2023). <https://doi.org/10.1109/TMI.2023.3264513>, <https://www.ncbi.nlm.nih.gov/pubmed/37018111>
7. Huang, J., Zhou, Y., Luo, Y., Liu, G., Guo, H., Yang, G.: Representing topological self-similarity using fractal feature maps for accurate segmentation of tubular structures. In: European Conference of Computer Vision 2024. pp. 143–160. *Computer Vision – ECCV 2024*, Springer Nature Switzerland (2025)
8. Isensee, F., Jaeger, P.F., Kohl, S.A.A., Petersen, J., Maier-Hein, K.H.: nnu-net: a self-configuring method for deep learning-based biomedical image segmentation. *Nature Methods* **18**(2), 203–211 (2021). <https://doi.org/10.1038/s41592-020-01008-z>, <https://www.ncbi.nlm.nih.gov/pubmed/33288961>
9. Jha, D., Smedsrud, P.H., Riegler, M.A., Halvorsen, P., de Lange, T., Johansen, D., Johansen, H.D.: Kvasir-seg: A segmented polyp dataset. In: *MultiMedia Modeling 2020*. pp. 451–462. *MultiMedia Modeling*, Springer International Publishing (2020). https://doi.org/10.1007/978-3-030-37734-2_37
10. Kirillov, A., Mintun, E., Ravi, N., Mao, H., Rolland, C., Gustafson, L., Xiao, T., Whitehead, S., Berg, A.C., Lo, W.Y., Dollár, P., Girshick, R.: Segment anything. 2023 IEEE/CVF International Conference on Computer Vision, ICCV pp. 3992–4003 (2023). <https://doi.org/10.1109/ICCV51070.2023.00371>
11. Lee, S., Kang, S., Shim, H.: Self-supervised vision transformers are efficient segmentation learners for imperfect labels (January 01 2024). <https://doi.org/10.48550/arXiv.2401.12535>, <https://ui.adsabs.harvard.edu/abs/2024arXiv240112535L>, the AAAI Conference on Artificial Intelligence 2024 Edge Intelligence Workshop (EIW)
12. Li, C., Liu, X., Li, W., Wang, C., Liu, H., Liu, Y., Chen, Z., Yuan, Y.: U-kan makes strong backbone for medical image segmentation and generation. *Proceedings of the AAAI Conference on Artificial Intelligence* **39**(5), 4652–4660 (2025). <https://doi.org/10.1609/aaai.v39i5.32491>, <https://ojs.aaai.org/index.php/AAAI/article/view/32491>
13. Li, L., Zhou, Y., Yang, G.: Robust source-free domain adaptation for fundus image segmentation. In: 2024 IEEE/CVF Winter Conference on Applications of Computer Vision (WACV). pp. 7825–7834 (2024). <https://doi.org/10.1109/wacv57701.2024.00766>
14. Li, Y., Wu, Y., Lai, Y., Hu, M., Yang, X.: Meddinov3: How to adapt vision foundation models for medical image segmentation? (September 01 2025). <https://doi.org/10.48550/arXiv.2509.02379>, <https://ui.adsabs.harvard.edu/abs/2025arXiv250902379L>
15. Liu, C., Chen, Y., Shi, H., Lu, J., Jian, B., Pan, J., Cai, L., Wang, J., Yu, J., Gao, Z., Zhang, X., Bai, L., Zhang, Y., Li, J., Bercea, C.I.,

- Ouyang, C., Chen, C., Xiong, Z., Wiestler, B., Wachinger, C., Duncan, J.S., Rueckert, D., Bai, W., Arcucci, R.: Does dinov3 set a new medical vision standard? benchmarking 2d and 3d classification, segmentation, and registration (September 01 2025). <https://doi.org/10.48550/arXiv.2509.06467>, <https://ui.adsabs.harvard.edu/abs/2025arXiv250906467L>, technical Report
16. Ma, J., He, Y., Li, F., Han, L., You, C., Wang, B.: Segment anything in medical images. *Nature Communications* **15**(1), 654 (2024). <https://doi.org/10.1038/s41467-024-44824-z>, <https://www.ncbi.nlm.nih.gov/pubmed/38253604>
 17. Noh, S., Lee, B.D.: A narrative review of foundation models for medical image segmentation: zero-shot performance evaluation on diverse modalities. *Quantitative Imaging in Medicine and Surgery* **15**(6), 5825–5858 (2025), <https://qims.amegroups.org/article/view/138057>
 18. Oquab, M., Darcet, T., Moutakanni, T., Vo, H., Szafraniec, M., Khalidov, V., Fernandez, P., Haziza, D., Massa, F., El-Nouby, A., Assran, M., Balbas, N., Galuba, W., Howes, R., Huang, P.Y., Li, S.W., Misra, I., Rabbat, M., Sharma, V., Synnaeve, G., Xu, H., Jegou, H., Mairal, J., Labatut, P., Joulin, A., Bojanowski, P.: Dinov2: Learning robust visual features without supervision (April 01 2023). <https://doi.org/10.48550/arXiv.2304.07193>, <https://ui.adsabs.harvard.edu/abs/2023arXiv230407193O>
 19. Ronneberger, O., Fischer, P., Brox, T.: U-net: Convolutional networks for biomedical image segmentation. In: *Medical Image Computing and Computer-Assisted Intervention (MICCAI 2015)*. pp. 234–241. *Lecture Notes in Computer Science*, Springer International Publishing (2015). https://doi.org/10.1007/978-3-319-24574-4_28, <http://arxiv.org/pdf/1505.04597>
 20. Schulthess, N., Konukoglu, E.: Anomaly detection by clustering dino embeddings using a dirichlet process mixture. In: *Medical Image Computing and Computer Assisted Intervention – MICCAI 2025*. pp. 46–56. Springer Nature Switzerland (2026)
 21. Siméoni, O., Vo, H.V., Seitzer, M., Baldassarre, F., Oquab, M., Jose, C., Khalidov, V., Szafraniec, M., Yi, S., Ramamonjisoa, M., Massa, F., Haziza, D., Wehrstedt, L., Wang, J., Darcet, T., Moutakanni, T., Sentana, L., Roberts, C., Vedaldi, A., Tolan, J., Brandt, J., Couprie, C., Mairal, J., Jégou, H., Labatut, P., Bojanowski, P.: Dinov3 (August 01 2025). <https://doi.org/10.48550/arXiv.2508.10104>, <https://ui.adsabs.harvard.edu/abs/2025arXiv250810104S>
 22. Sun, J., Chen, K., He, Z., Ren, S., He, X., Liu, X., Peng, C.: Medical image analysis using improved sam-med2d: segmentation and classification perspectives. *BMC Medical Imaging* **24**(1), 241 (2024). <https://doi.org/10.1186/s12880-024-01401-6>, <https://www.ncbi.nlm.nih.gov/pubmed/39285324>
 23. Wahd, A.S., Felfeliyan, B., Zhou, Y., Ghosh, S., McArthur, A., Zhang, J., Jaremko, J.L., Hareendranathan, A.: Sam2rad: A segmentation model for medical images with learnable prompts. *Computers in Biology and Medicine* **187**, 109725 (2025). <https://doi.org/10.1016/j.compbiomed.2025.109725>, <https://www.ncbi.nlm.nih.gov/pubmed/39914197>
 24. Wang, S., Safari, M., Hu, M., Li, Q., Chang, C.W., Qiu, R.L., Yang, X.: Dinov3 with test-time training for medical image registration (August 01 2025). <https://doi.org/10.48550/arXiv.2508.14809>, <https://ui.adsabs.harvard.edu/abs/2025arXiv250814809W>
 25. Xu, G., Udupa, J.K., Lu, W., Zhang, Y.: Exploiting dinov3-based self-supervised features for robust few-shot medical image segmen-

- tation (January 01 2026). <https://doi.org/10.48550/arXiv.2601.08078>, <https://ui.adsabs.harvard.edu/abs/2026arXiv260108078X>, 36 pages, 11 figures
26. Yang, S., Wang, H., Xing, Z., Chen, S., Zhu, L.: Segdino: An efficient design for medical and natural image segmentation with dino-v3 (August 01 2025). <https://doi.org/10.48550/arXiv.2509.00833>, <https://ui.adsabs.harvard.edu/abs/2025arXiv250900833Y>
 27. Yeung, M., Sala, E., Schonlieb, C.B., Rundo, L.: Focus u-net: A novel dual attention-gated cnn for polyp segmentation during colonoscopy. *Comput Biol Medical* **137**, 104815 (2021). <https://doi.org/10.1016/j.compbimed.2021.104815>, <https://www.ncbi.nlm.nih.gov/pubmed/34507156>
 28. Zhang, X., Chen, E.Z., Zhao, L., Chen, X., Liu, Y., Maihe, B., Duncan, J.S., Chen, T., Sun, S.: Adapting vision foundation models for real-time ultrasound image segmentation. In: *Medical Image Computing and Computer Assisted Intervention – MICCAI 2025*. pp. 24–34. Springer Nature Switzerland (2026). https://doi.org/10.1007/978-3-032-04971-1_3
 29. Zheng, X., Zhang, Y., Zhang, H., Liang, H., Bao, X., Jiang, Z., Lao, Q.: Curriculum prompting foundation models for medical image segmentation. In: *Medical Image Computing and Computer Assisted Intervention – MICCAI 2024*. pp. 487–497. Springer Nature Switzerland (2024)
 30. Zhou, Y., Li, L., Lu, L., Xu, M.: nnwnet: Rethinking the use of transformers in biomedical image segmentation and calling for a unified evaluation benchmark. In: *2025 IEEE/CVF Conference on Computer Vision and Pattern Recognition (CVPR)*. pp. 20852–20862 (2025). <https://doi.org/10.1109/cvpr52734.2025.01942>